Molecular Cell, Volume *50*

Supplemental Information

Control of Protein Quality and Stoichiometries by N-Terminal Acetylation and the N-End Rule Pathway

Anna Shemorry, Cheol-Sang Hwang, and Alexander Varshavsky

Supplemental Information Inventory:

Figures S1-S5 (conceptually linked to the main Figures 1-5) and their legends.

Supplemental Experimental Procedures.

Tables S1 and S2.

Supplemental References.

Figure S1 refers to Figures 1, 2 and 4.

Figure S2 refers to Figures 1 and 5.

Figure S3 refers to Figure 1.

Figure S4 refers to Figures 1 and 3.

Figure S5 refers to Figures 1-3.

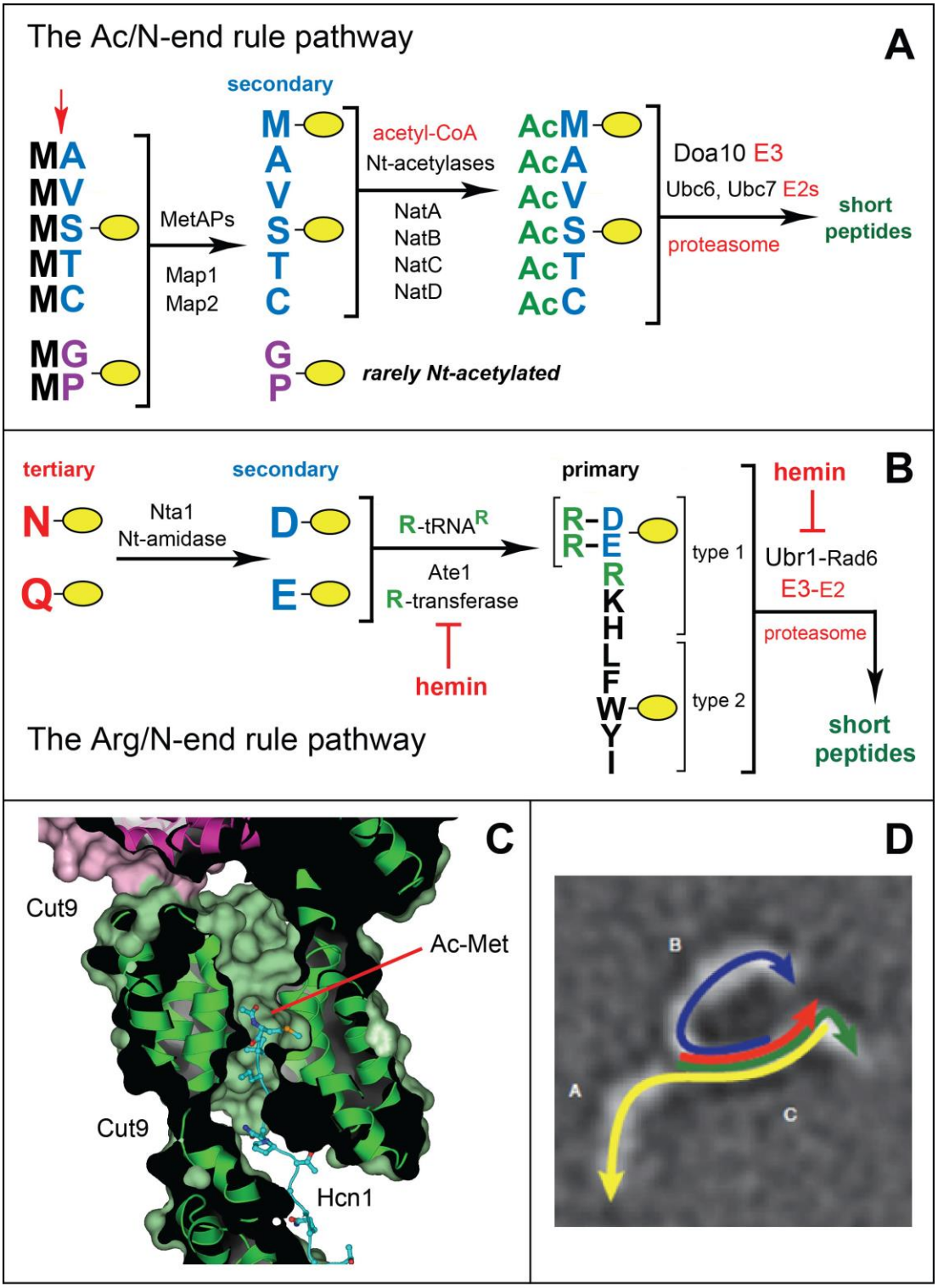

Figure S1, Shemorry et al.

Figure S1. The Ac/N-End Rule Pathway, the Arg/N-End Rule Pathway, and the Steric Sequestration of N^{α}-Terminally Acetylated N-Termini of Cellular Proteins.

(A) The Ac/N-end rule pathway in the yeast *Saccharomyces cerevisiae* (Hwang et al., 2010b; Varshavsky, 2011). N-terminal residues are indicated by single-letter abbreviations for amino acids. A yellow oval denotes the rest of a protein substrate. E3 ubiquitin (Ub) ligases of the

N-end rule pathway are called N-recognins. The Doa10 E3 N-recognin physically binds to N^{α}-terminally acetylated (Nt-acetylated) polypeptides and contributes to the in vivo degradation of previously examined Nt-acetylated proteins (Hwang et al., 2010b). In the present study, we identified Not4 as a putative second N-recognin of the Ac/N-end rule pathway (Figure 2 and Discussion). Red arrow on the left indicates the removal of N-terminal Met by Met-aminopeptidases (MetAPs). N-terminal Met is retained if a residue at position 2 is nonpermissive (too large) for MetAPs ((Varshavsky, 2011) and references therein). If the retained N-terminal Met or N-terminal Ala, Val, Ser, Thr, and Cys are followed by acetylation-permissive residues, the cited N-terminal residues are usually Nt-acetylated by the Nt-acetylases NatA-NatD, the bulk of which is associated with the ribosomes (Arnesen et al., 2009; Starheim et al., 2012; Van Damme et al., 2012). Although second-position Gly or Pro can be made N-terminal by MetAPs and although the Doa10 E3 N-recognin can recognize Nt-acetylated Gly or Pro (Hwang et al., 2010b), few proteins with N-terminal Gly or Pro are Nt-acetylated. See Figure S2 for a summary of Nt-acetylation vis-à-vis specific N-terminal residues. The Nt-acetylation-mediated N-degrons are called Ac/N-degrons, to distinguish them from other N-degrons. The term "secondary" refers to the requirement for a modification (Nt-acetylation) of a destabilizing N-terminal residue before a protein can be recognized by a cognate N-recognin. Physiological functions of the Ac/N-end rule pathway are discussed in the main text.

(B) The Arg/N-end rule pathway in *S. cerevisiae* (Varshavsky, 2011). The Ubr1/Rad6 E3-E2 N-recognin Ub ligase directly recognizes (binds to) the "primary" destabilizing N-terminal residues Arg, Lys, His, Leu, Phe, Tyr, Trp and Ile. In contrast, N-terminal Asn, Gln, Asp, and Glu (as well as Cys, under some metabolic conditions) are destabilizing owing to their preliminary enzymatic modifications. These include the Nt-deamidation of N-terminal Asn and Gln by the Nta1 Nt-amidase and the Nt-arginylation of N-terminal Asp and Glu by the Ate1 arginyltransferase (R-transferase), which can also Nt-arginylate oxidized Cys, either Cys-sulfinate or Cys-sulfonate. These derivatives of N-terminal Cys can form in cells that produce nitric oxide (NO) and may also form in *S. cerevisiae*. One aspect of the *S. cerevisiae* Arg/N-end rule pathway that is not illustrated in this diagram is a physical and functional interaction between the Ubr1 E3 of the Arg/N-end rule pathway and the Ufd4 E3 of the previously characterized Ub-fusion-degradation (UFD) pathway. Specifically, the targeting apparatus of the Arg/N-end rule pathway comprises a physical complex of the RING-type E3 Ubr1 N-recognin and the HECT-type E3 Ufd4, together with their cognate E2 enzymes Rad6 and Ubc4 (or Ubc5), respectively (Hwang et al., 2010a). In addition to its two distinct binding sites that recognize type 1 (basic) and type 2 (bulky hydrophobic) destabilizing N-terminal residues, the *S. cerevisiae* Ubr1 N-recognin also contains (similarly to its counterparts in multicellular eukaryotes) at least one more binding site, which recognizes substrates that are targeted through their internal (non-N-terminal) degradation signals. One example of such a substrate is the Cup9 transcriptional repressor (Byrd et al., 1998; Turner et al., 2000; Xia et al., 2008a). Polyubiquitylated N-end rule substrates are processively destroyed to short peptides by the 26S proteasome. Hemin (Fe^{3+}-heme) binds to R-transferase and inhibits its Nt-arginylation activity. Hemin also binds to Ubr1 and alters its functional properties, in ways that remain to be understood (Hu et al., 2008).

Regulated degradation of specific proteins by the Arg/N-end rule pathway mediates the sensing of heme, NO, oxygen and short peptides; the selective elimination of misfolded proteins; the regulation of DNA repair; the cohesion/segregation of chromosomes; the signaling by transmembrane receptors; the control of peptide import; the regulation of apoptosis, meiosis, viral and bacterial infections, fat metabolism, cell migration, actin filaments, cardiovascular development, spermatogenesis, neurogenesis, and memory; the functioning of adult organs, including the brain, muscle, testis, and pancreas; and the regulation of leaf and shoot development, leaf senescence, and

many other functions in plants ((Brower and Varshavsky, 2009; Choi et al., 2010; Dougan et al., 2011; Eisele and Wolf, 2008; Gibbs et al., 2011; Graciet and Wellmer, 2010; Heck et al., 2010; Hu et al., 2005; Hu et al., 2008; Hwang et al., 2009; Hwang et al., 2010a; Hwang et al., 2011; Hwang and Varshavsky, 2008; Kurosaka et al., 2010; Kwon et al., 2002; Lee et al., 2012; Lee et al., 2005; Licausi et al., 2011; Matta-Camacho et al., 2010; Mogk et al., 2007; Piatkov et al., 2012a; Piatkov et al., 2012b; Prasad et al., 2010; Rao et al., 2001; Sasidharan and Mustroph, 2011; Tasaki et al., 2012; Varshavsky, 1996, 2011; Wang et al., 2009; Xia et al., 2008b; Zenker et al., 2005; Zhang et al., 2010a) and references therein).

(C) Steric shielding of the Nt-acetylated N-terminal residue of a subunit in a protein complex. Shown here is a part of the crystal structure, by the Barford laboratory, of a complex between the Hcn1 and Cut9 subunits of the *Schizosaccharomyces pombe* APC/C Ub ligase (Zhang et al., 2010b). In this structure, the (indicated) Nt-acetylated N-terminal Met residue of Hcn1 is enclosed within a deep cleft formed by the Cut9 subunit, in the heterotetramer of Hcn1 and Cut9. The N-terminal region of Hcn1 is shown in cyan as a stick model, and Cut9 is depicted as a cut-out surface representation, to show the chamber's interior (Zhang et al., 2010b).

(D) Model of interactions, based on single-particle electron microscopy by the Hughson laboratory, among the subunits Cog1-Cog4 that form a specific subcomplex of the S. cerevisiae COG complex (Lees et al., 2010). The head of an arrow and its blunt end indicate the C-terminus and the N-terminus of a protein, respectively. The green, red, yellow, and blue arrows denote Cog1, Cog2, Cog3 and Cog4, respectively (Lees et al., 2010). Figure S1 refers to Figures 1, 3 and 5.

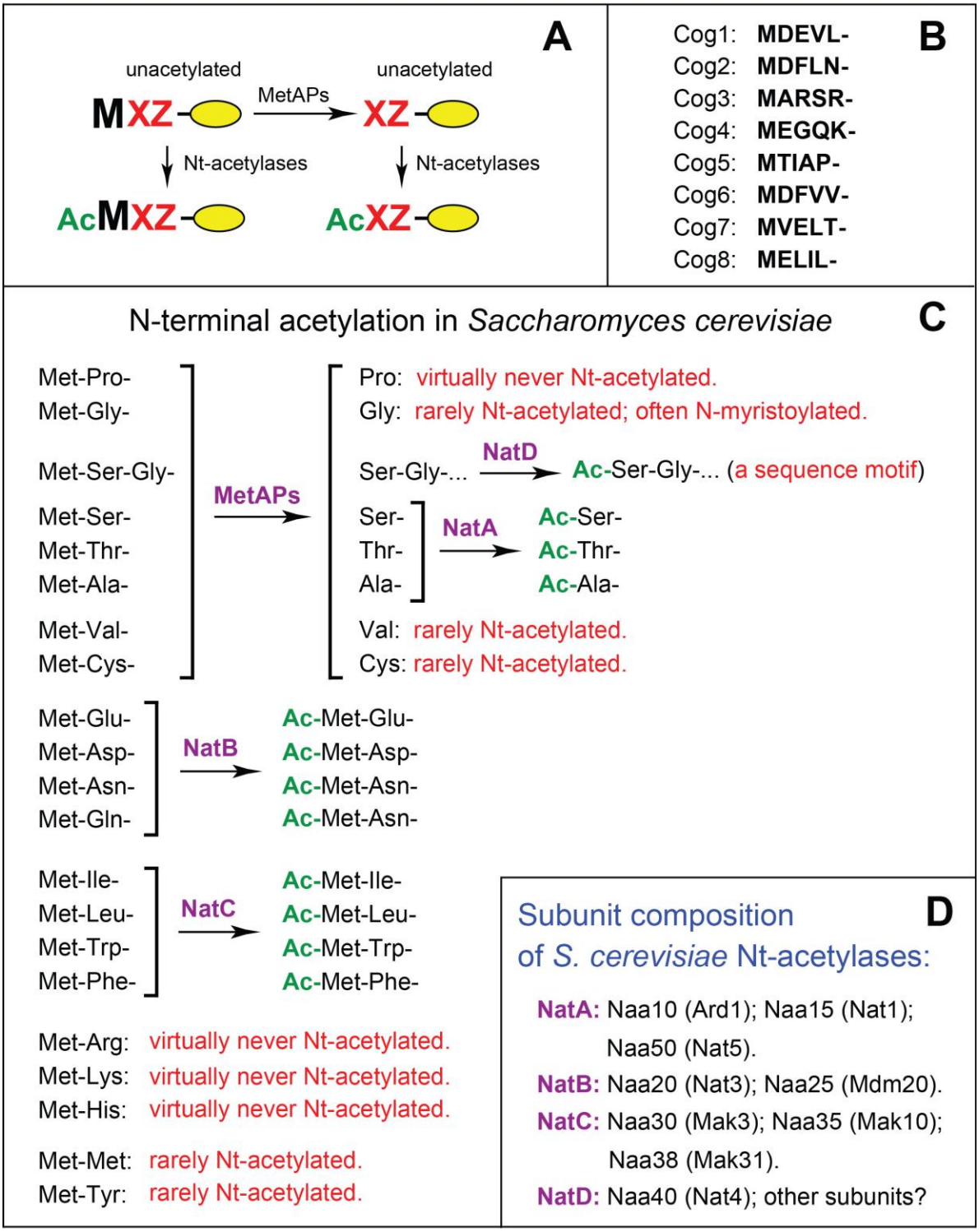

Fig. S2, Shemorry et al.

Figure S2. N-terminal Processing of Nascent Proteins, the N-termini of COG Subunits, and the N^{α}-Terminal Acetylation in *S. cerevisiae*.

(A) N-terminal processing of nascent cellular proteins by N^{α}-terminal acetylases (Nt-acetylases) and Met-aminopeptidases (MetAPs). "Ac" denotes the N^{α}-terminal acetyl moiety.

M, Met. X and Z, single-letter abbreviations for any amino acid residue. Yellow ovals denote the rest of a protein.

(B) The first 5 encoded N-terminal residues of the Cog1-Cog8 subunits of the Conserved Oligomeric Golgi (COG) complex in *S. cerevisiae* (Miller and Ungar, 2012; Sztul and Lupashin, 2009). The Nt-acetylation status of the seven COG subunits (Cog2-Cog8) other than MD-Cog1^{wt} remains to be determined. Save for Cog3, all of these subunits are candidates for Nt-acetylation in wild-type (wt) cells.

(C) Substrate specificities and subunit compositions of *S. cerevisiae* Nt-acetylases. This compilation is derived from data in the literature ((Arnesen et al., 2009; Helbig et al., 2010; Polevoda and Sherman, 2003; Starheim et al., 2012; Van Damme et al., 2012) and references therein). The present paper uses the revised nomenclature for specific subunits of Nt-acetylases (Polevoda et al., 2009) and cites the older names of these subunits in parentheses. Figure S2 refers to Figures 1 and 6.

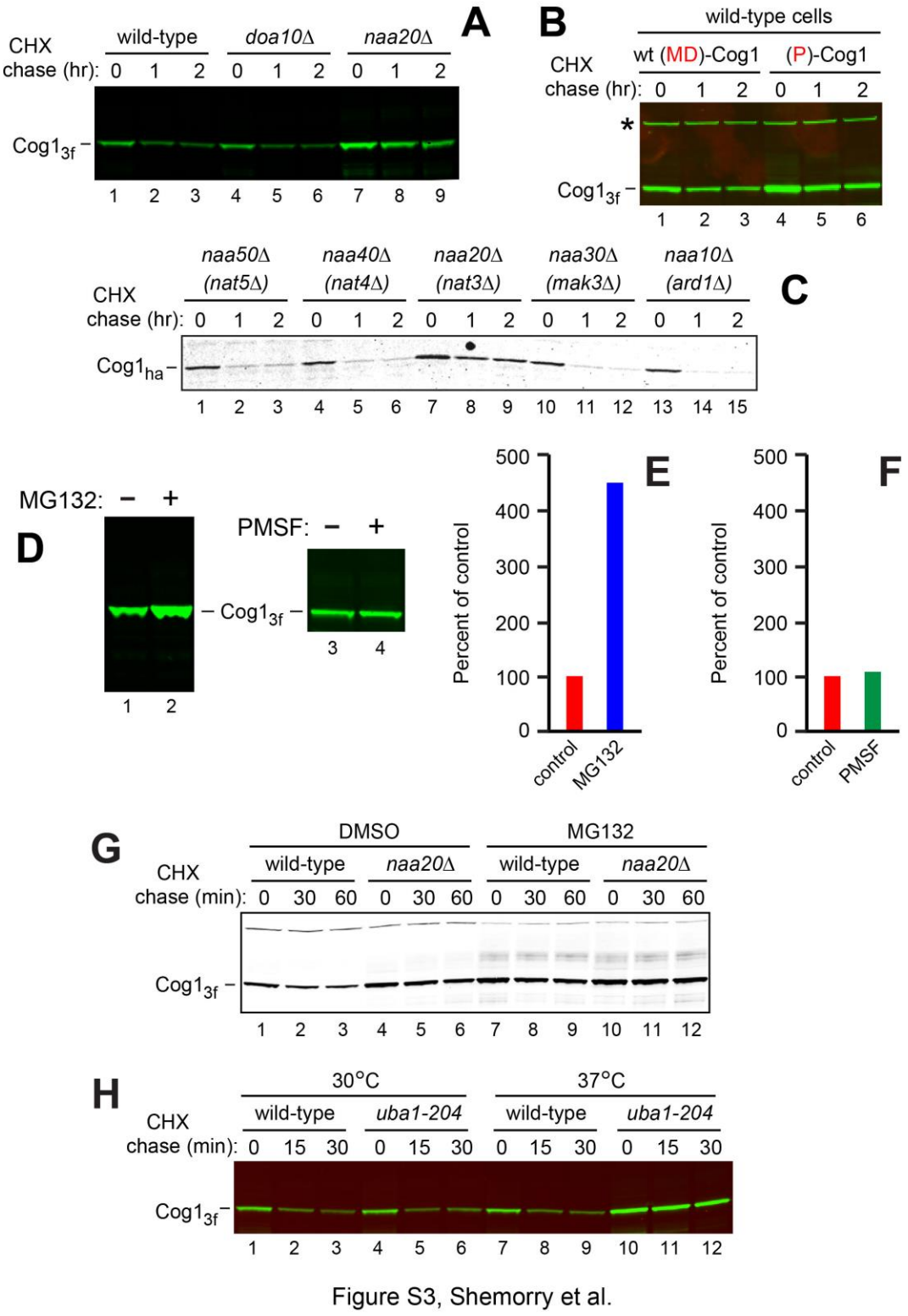

Figure S3, Shemorry et al.

Figure S3. Degradation of Cog1 by the Ac/N-End Rule Pathway.

(A) Cycloheximide (CHX)-chases (related to the ones described in Figure 1) were carried out at 30°C with wt (lanes 1-3), *doa10Δ* (lanes 4-6) and *naa20Δ* (*nat3Δ*) (lanes 7-9) *S. cerevisiae* strains that expressed wt Cog1, termed MD-Cog1^{wt}, which was C-terminally tagged with three flag

epitopes. At the indicated times of chase, proteins in cell extracts were fractionated by SDS-PAGE and assayed by immunoblotting with anti-Flag antibody.

(B) CHX-chases as in A, with wt cells that expressed MD-Cog1^{wt} (lanes 1-3) or its non-Nt-acetylatable P-Cog1 mutant (lane 4-6), both of which were C-terminally tagged with three flag epitopes. See the main text for descriptions of P-Cog1. Asterisk on the left denotes a crossreacting protein.

(C) CHX-chases as in A, with MD-Cog1^{wt} C-terminally ha-tagged and examined in *naa50Δ* (*nat5Δ*) (lanes 1-3), *naa40Δ* (*nat4Δ*) (lanes 4-6), *naa20Δ* (*nat3Δ*) (lanes 7-9), *naa30Δ* (*mak3Δ*) (lanes 10-12), and *naa10Δ* (*ard1Δ*) (lanes 13-15) S. cerevisiae strains. Each of these strains lacked the activity of a specific Nt-acetylase (see Figure S2C), including the cognate (for MD-Cog1^{wt}) NatB Nt-acetylase (lanes 7-9).

(D) Left panel: Expression of MD-Cog1^{wt} C-terminally tagged with three flag epitopes in *pdr5Δ S. cerevisiae*. Cells were incubated for 1 hr in SD medium containing either 0.5% dimethylsulfoxide (DMSO) (the solvent for a stock solution of the proteasome inhibitor MG132) (lane 1), or both 50 μM MG132 and 0.5% DMSO (lane 2). The incubation was followed by preparation of extracts, SDS-PAGE and immunoblotting with anti-Flag antibody. Right panel: same procedures as in experiments of the left panel but with *erg6Δ S. cerevisiae* incubated in SD containing either 1% isopropanol (the solvent for a stock solution of phenylmethylsulfonyl fluoride (PMSF), an inhibitor of serine proteases) (lane 1), or both 1 mM PMSF and 1% isopropanol (lane 2).

(E) Quantification of data in D, left panel.

(F) Quantification of data in D, right panel.

(G) CHX-chases with wt (lanes 1-3, 7-9) or *naa20Δ* (*nat3Δ*) (lanes 4-6, 10-12) *S. cerevisiae* strains expressing MD-Cog1^{wt} C-terminally tagged with three flag epitopes. Cells were grown for 3 hrs in SD medium containing 0.003% SDS (to allow for the entry of MG132) and either 0.5% DMSO (control, lanes 1-6) or both 50 μM MG132 and 0.5% DMSO. Note the metabolic stabilization of MD-Cog1^{wt} in wild-type cells by MG132 (lanes 1-3 vs. lanes 7-9) and the metabolic stabilization of MD-Cog1^{wt} in *naa20Δ* cells (lacking the NatB Nt-acetylase) irrespective of the absence or presence of MG132 (lanes 4-6 vs. lanes 10-12).

(H) CHX-chases with either wt or *uba1-204 S. cerevisiae* (the latter containing a temperature-sensitive mutant of the Ub-activating (E1) enzyme (Ghaboosi and Deshaies, 2007)) expressing MD-Cog1^{wt} C-terminally tagged with three flag epitopes. Lanes 1-3, wt cells at 30°C. Lanes 4-5, *uba1-204* cells at 30°C. Lanes 7-8, same as in lanes 1-3 but at 37°C (nonpermissive temperature for *uba1-204* cells). Lanes 10-12, same as lanes 4-6 but at 37°C. Note the metabolic stabilization of MD-Cog1^{wt} in *uba1-204* cells at 37°C (lanes 10-12). Figure S3 refers to Figure 1.

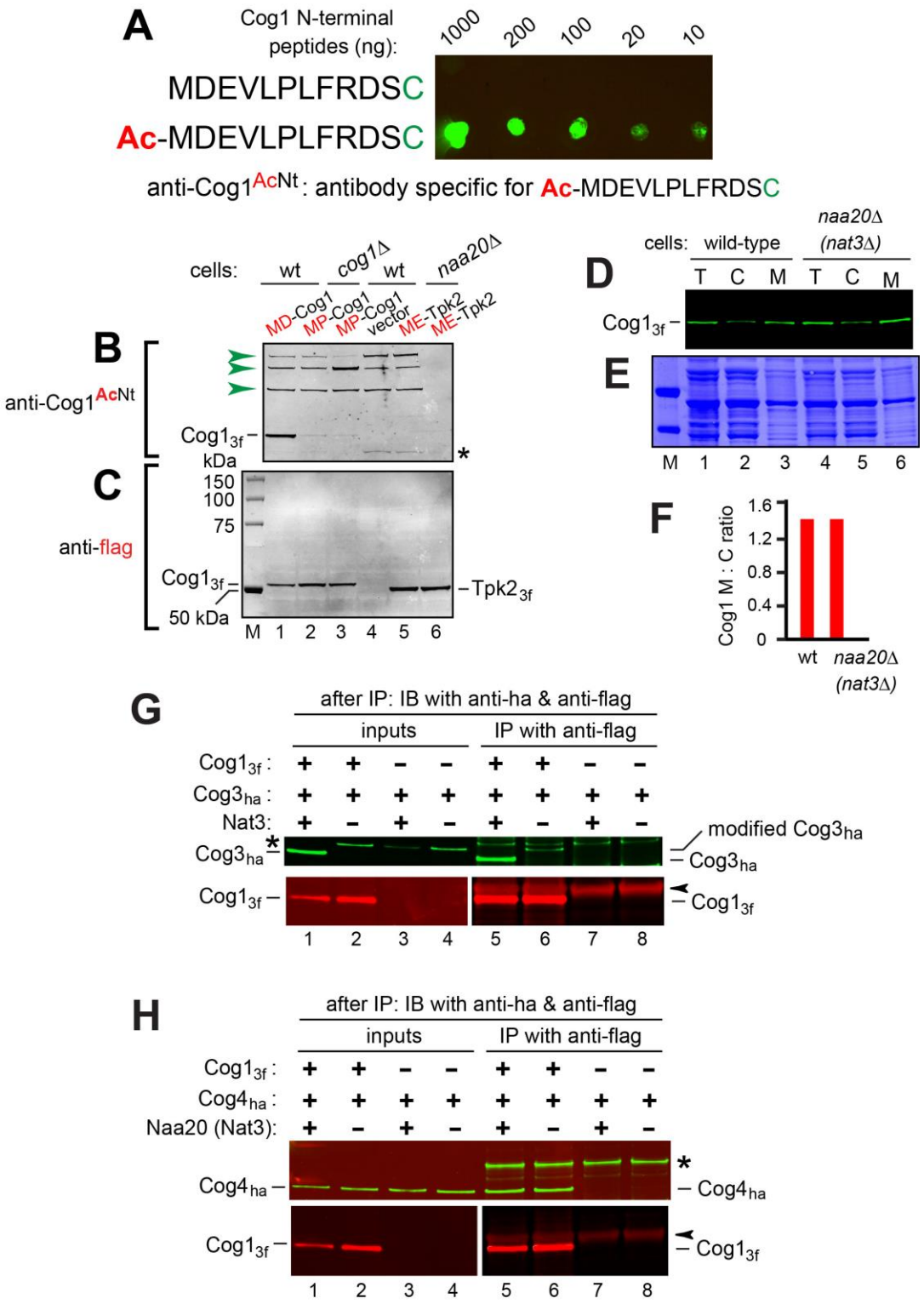

Figure S4, Shemorry et al.

Figure S4. Antibody Specific for Nt-Acetylated Cog1, and Interactions of Nt-Acetylated and Unacetylated Cog1 with Subunits of the COG Complex or with Membranes.

(A) Characterization of the anti-^{AcNt}Cog1 antibody using a dot immunoassay. Increasing amounts of the Nt-acetylated Ac-MDEVLPLFRDSC peptide and its non-acetylated counterpart

MDEVLPLFRDSC were spotted onto a nitrocellulose membrane, followed by immunoblotting with the rabbit anti-^{AcNt}Cog1 antibody that was raised against the Ac-MDEVLPLFRDSC peptide and was then affinity-purified both "positively" (against Ac-MDEVLPLFRDSC) and "negatively" (against MDEVLPLFRDSC) (see Extended Experimental Procedures).

(B) Wt, *cog1Δ*, and *naa20Δ* (*nat3Δ*) S. cerevisiae strains overexpressed either MD-Cog1^{wt}, P-Cog1, or ME-Tpk2 (an Nt-acetylated protein whose N-terminal sequence is different from that of MD-Cog1^{wt}; a negative control) from the P_{CUP1} promoter on low copy plasmids. Equal amounts of total protein in the extracts were fractionated by SDS-PAGE and immunoblotted with the anti-^{AcNt}Cog1 antibody. Lane 1, MD-Cog1^{wt} (C-terminally tagged with three flag epitopes) was expressed in wt cells. Lane 2, same as in lane 1 but the identically tagged P-Cog1 (MP-Cog1). Lane 3, same as in lane 2 but in *cog1Δ* cells. Lane 4, same as in lane 1 but vector alone (no exogenously expressed MD-Cog1^{wt}). Lane 5, ME-Tpk2 (C-terminally tagged with three flag epitopes) was expressed in wt cells. Lane 6, same as in lane 5 but ME-Tpk2 was expressed in *naa20Δ* (*nat3Δ*) cells lacking the cognate NatB Nt-acetylase.

Anti-^{AcNt}Cog1 detected the band of Nt-acetylated MD-Cog1^{wt} in lane 1. Consistently, there was virtually no signal in other lanes, except for the barely detectable band in lanes 4 and 5 (marked by asterisk on the right) that is likely to be the endogenous Nt-acetylated MD-Cog1^{wt} (endogenous MD-Cog1^{wt} was expressed at levels significantly below those of exogenous MD-Cog1^{wt}). Consistent with the absence of three flag epitopes in the endogenous MD-Cog1^{wt}, its band migrated faster than the band of the exogenous (tagged) MD-Cog1^{wt} (lane 1 vs. lanes 4 and 5). Note the absence of crossreaction of anti-^{AcNt}Cog1 with Nt-acetylated ME-Tpk2 in wt cells (lane 5). The anti-^{AcNt}Cog1 antibody also detected proteins larger than MD-Cog1^{wt}; they are marked by green arrowheads on the left. These proteins were not derivatives of MD-Cog1^{wt}, as they were present in cells not expressing MD-Cog1^{wt} (lane 4). The three proteins were Nt-acetylated by NatB, as they were absent in *naa20Δ* (*nat3Δ*) cells (lane 6). A likely and parsimonious interpretation is that the anti-^{AcNt}Cog1 antibody detected three specific Nt-acetylated proteins whose cognate Nt-acetylase (NatB) is the same as the one that Nt-acetylates MD-Cog1^{wt} and whose N-terminal sequences are sufficiently close to that of MD-Cog1^{wt} to have resulted in a crossreaction.

(C) Same as in B, but the same membrane was re-probed with anti-flag antibody, to detect the bulk of triply flag-tagged MD-Cog1^{wt} and ME-Tpk2.

(D) Equal amounts of total detergent-free cell extracts from wt or *naa20Δ* (*nat3Δ*) *S. cerevisiae* were fractionated to yield the cytosolic (C) and membrane (M) fractions, followed by SDS-PAGE and immunoblotting with anti-flag antibody to detect the triply flag-tagged MD-Cog1^{wt}. Lanes 1-3, wt total (T) extract and its C and M fractions, respectively. Lanes 4-6, same as in lanes 1-3 but from *naa20Δ* (*nat3Δ*) cells.

(E) Coomassie Blue staining of membrane probed by anti-flag in D.

(F) Quantification of the ratio of MD-Cog1^{wt} in the membrane versus cytosolic fractions in panel D, using Odyssey (Li-Cor) (see Extended Experimental Procedures).

(G) Coimmunoprecipitation of MD-Cog1^{wt} and Cog3 in the presence and absence of Nt-acetylation. Wt and *naa20Δ* (*nat3Δ*) *S. cerevisiae* strains carried either a P_{CUP1} promoter-containing low copy plasmid, or the otherwise identical plasmid expressing MD-Cog1^{wt} (C-terminally tagged with three flag epitopes), or the plasmid expressing Cog3 (C-terminally ha-tagged), in the indicated combinations of test proteins and genetic backgrounds of strains in which they were expressed. Extracts from these strains were immunoprecipitated using anti-flag beads, followed by SDS-PAGE and immunoblotting with anti-ha (to detect Cog3; the upper panel, green color) or with anti-flag (to detect MD-Cog1^{wt}; the lower panel, red color). As described in the main text, most Cog3 in *naa20Δ* (*nat3Δ*) cells was converted into a derivative of lower electrophoretic mobility, indicated on the right as "modified Cog3". The asterisk on the left

indicates a protein crossreacting with anti-ha antibody. The arrowhead on the right marks the position of the heavy IgG chain, above the band of immunoprecipitated MD-Cog1^{wt}.

(H) Same as in G (including the same notations), but coimmunoprecipitation of MD-Cog1^{wt} (C-terminally tagged with three flag epitopes) and Cog4 (C-terminally ha-tagged). The asterisk in the top panel on the right indicates a protein crossreacting with anti-ha. Figure S4 refers to Figures 1 and 4.

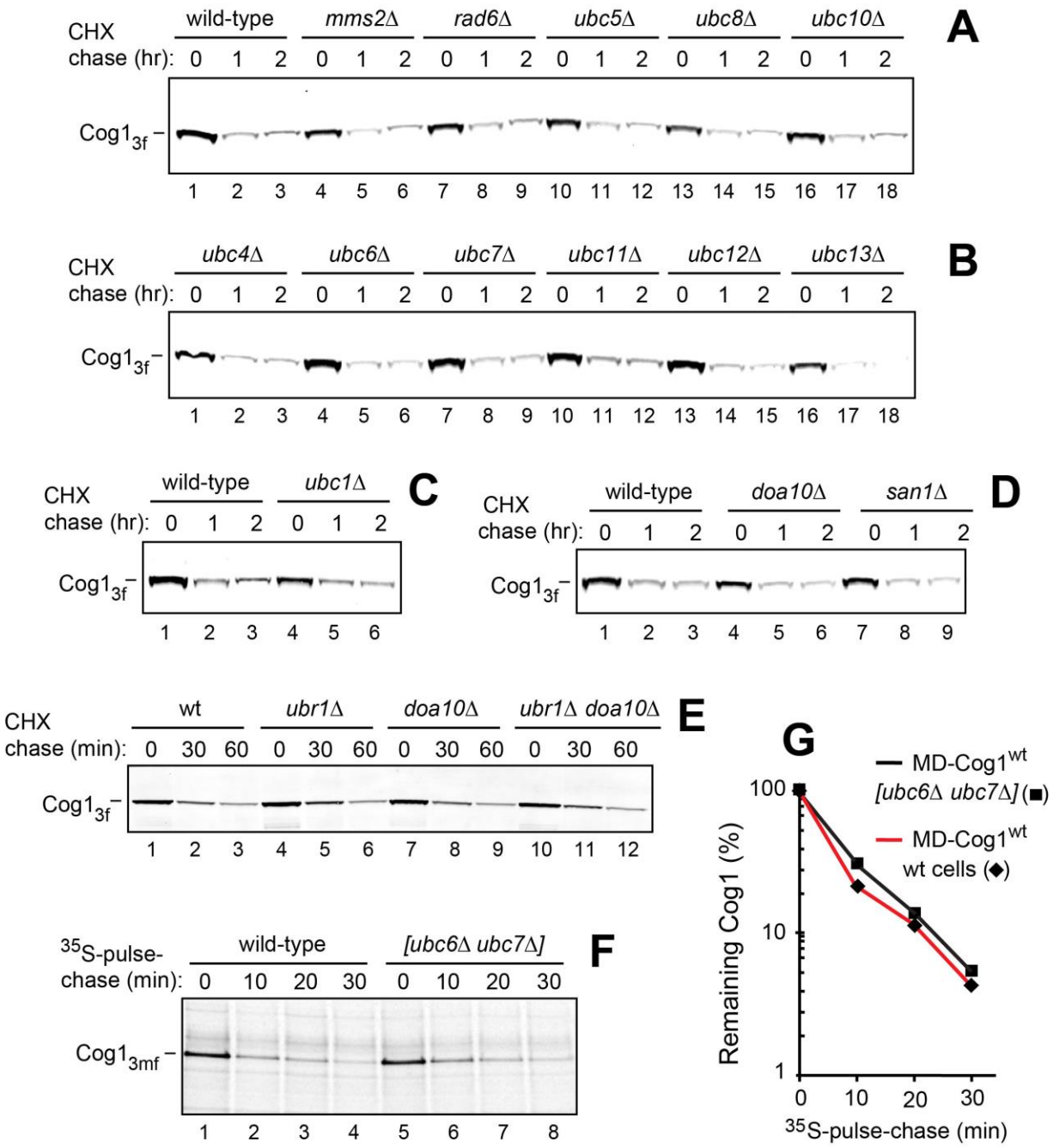

Figure S5, Shemorry et al.

Figure S5. Degradation of MD-Cog1^{wt} by the Ac/N-End Rule Pathway in *S. cerevisiae* Mutants Lacking Specific E2 or E3 enzymes.

(A) CHX-chases with yeast mutants in specific Ub-conjugating (E2) enzymes that expressed MD-Cog1^{wt} C-terminally tagged with three flag epitopes. Wt *S. cerevisiae* (lanes 1-3) and *mms2Δ* (lanes 4-6), *rad6Δ* (lanes 7-9), *ubc5Δ* (lanes 10-12), *ubc8Δ* (lanes 13-15), and *ubc10Δ* (lanes 16-18) mutants.

(B) Same as in A but with *S. cerevisiae* mutants *ubc4Δ* (lanes 1-3), *ubc6Δ* (lanes 4-6), *ubc7Δ* (lanes 7-9), *ubc11Δ* (lanes 10-12), *ubc12Δ* (lanes 13-15), and *ubc13Δ* (lanes 16-18).

(C) Same as in A but with wt (lanes 1-3) and *ubc1Δ* (lanes 4-6) *S. cerevisiae*.

(D) CHX-chases with mutants in two specific E3 enzymes. Same as in A but with wt (lanes 1-3), *doa10Δ* (lanes 4-6), and *san1Δ* (lanes 7-9) *S. cerevisiae* strains.

(E) Same as in D but the chases for 30 and 60 min with wt (lanes 1-3), *ubr1Δ* (lanes 4-6), *doa10Δ* (lanes 7-9), and double-mutant *ubr1Δ doa10Δ* (lanes 10-12) *S. cerevisiae* strains.

(F) Lanes 1-4, ^{35}S-pulse chase with wt *S. cerevisiae* and MD-Cog1^{wt} (C-terminally tagged with three flag epitopes modified to contain a Met residue in each epitope, to increase ^{35}S in Cog1; see Extended Experimental Procedures). Lanes 5-8, same as lanes 1-4 but with a double mutant *ubc6Δ ubc7Δ*.

(G) Quantification of ^{35}S-pulse-chase data in F.

SUPPLEMENTAL EXPERIMENTAL PROCEDURES

Yeast Strains, Media, and Genetic Techniques

S. cerevisiae strains used in this study are described in Table S1. Standard techniques (Ausubel et al., 2010; Sherman, 1991) were employed for strain construction and transformation. *S. cerevisiae* media included YPD (1% yeast extract, 2% peptone, 2% glucose; only most relevant components are cited); SD medium (0.17% yeast nitrogen base, 0.5% ammonium sulfate, 2% glucose); and synthetic complete (SC) medium (0.17% yeast nitrogen base, 0.5% ammonium sulfate, 2% glucose), plus a drop-out mixture of compounds required by a given auxotrophic strain. The COG1-3HA strains were made by standard PCR of the 3HA-HIS3MX6 module (Longtine et al., 1998) targeted to the 3' coding region of COG1. The PCR product was transformed into BY4742, BY17299, and BY15546 to create ASY101, ASY102, and ASY103, respectively. The double mutant *ubc6Δubc7Δ* (ASY104) was made by transforming BBY67.3 with a PCR product of the KanMX6 module (Longtine et al., 1998) targeted to the 5' and 3' regions of UBC7, thereby replacing the ORF of Ubc7 with KanMX6. The ASY105 strain was made by the standard integration of a PCR fragment derived from pFA6a-13MYC with the HIS3MX6 marker targeted to the 3' end of the *COG1* gene. Proper tagging of *COG1* and its product was verified by PCR and immunoblotting with anti-myc antibody. The resulting ASY105 strain was transformed with pAS118 or the control YEPlac181 plasmid (Table S2). E1, E2, E3 and Nt-acetylase mutant strains used in this study were from the Varshavsky lab stock (CHY345, CHY346, BBY67.3), the T. Sommer lab stock (YW05), the Deshaies lab stock (RJD3268, RJD3269) or all others from Open Biosystems. Strains used in the proteasome and vacuole inhibitor studies were obtained from Open Biosystems (BY10568) or from the Varshavsky lab stock (JD52, CHY49). The *cog1Δ* mutant (BY14589) was obtained from Open Biosystems.

Construction of Plasmids

The *S. cerevisiae* Cog1-coding sequence was amplified by PCR from genomic DNA and the triple flag-coding sequence was then added by PCR. Additional Met-coding sequences were added in between the Cog1-coding sequence and the triple flag-coding sequence to increase the labeling of MD-Cog1^{wt} with ^{35}S-Met. The 3 extra Met-coding DNA sequences were separated by short Gly-Ser linker sequences, the complete Met-enriching sequence being MSGMGAM. pAS101 was constructed by ligating the BamHI/Not1 digested PCR fragment of Cog1-3flag DNA into the low-copy (CEN) plasmid pRS316 with the P_{CUP1} promoter (p316Cup1). pAS117 was made by standard site-directed mutagenesis of pAS101 to insert a coding sequence for proline (P) in between the initiator Met (M) and Asp (D). pAS105 was made by amplifying the Cog1-coding sequence with a sequence encoding a single C-terminal ha tag and ligating this PCR product into the BamHI/NotI-cut p316Cup1 plasmid. pAS118 was made by standard point mutagenesis of pAS105 to mutate the aspartic acid (D) coding sequence to lysine (K). pAS102 was made by adding the 3flag sequence to the 3' end of the Cog2 PCR product and ligating that product into p316Cup1. pAS115 was made by inserting the Cog2-3f sequence and the Cog3-HA sequence on opposite sides of the $P_{GAL1/10}$ bidirectional promoter. pAS116 was made by inserting the Cog4-ha-coding sequence into pRS425Gal1/10. pAS118 was made by ligating the XbaI/PstI-derived, PCR-produced DNA fragment into XbaI/PstI-cut pRB208.

To construct pAS112 (Table S2), the *S. pombe HCN1* coding sequence was amplified from pGAD424-Hcn1. The triple flag-coding DNA sequence was then added to the 3' region of *HCN1*. The resulting PCR-produced DNA fragment was ligated into the high copy plasmid pRS423 (Ausubel et al., 2010) containing the P_{CUP1} promoter. The same PCR fragment from pAS112 was ligated into p413Met25 to produce pAS113. The *S. cerevisiae* DNA encoding Cdc26 was amplified

from genomic DNA and the triple flag-coding DNA sequence was added by PCR. The resulting DNA fragment was cloned into pRS423 as described above to produce pAS119. DNA encoding *S. pombe* Cut9 was amplified from pGAD424-Cut9, and the triple flag-coding DNA sequence was added to the 3' region of *CUT9* by PCR. The resulting DNA fragment was ligated into the high copy pRS425 plasmid containing the P_{GAL1} promoter, yielding pAS114.

Cycloheximide Chase Degradation Assays

S. cerevisiae were grown to A_{600} of 0.8 to 1.0 in plasmid-maintaining (selective) liquid media at 30°C, followed by treatment with cycloheximide (CHX), at the final concentration of 0.1 mg/ml. At indicated times, cell samples (corresponding to 1 ml of cell suspension at A_{600} of 1) were harvested by centrifugation for 1 min at 11,200*g*, and resuspended in 1 ml of 0.2 M NaOH, for 20 min on ice, or for 5 min at room temperature, followed by centrifugation for 1 min at 11,200*g*. Pelleted cells were resuspended in 50 µl of 1X LDS buffer (Invitrogen, Carlsbad, CA) with 1X reducing agent and 1x protease inhibitor cocktail "for use with fungal and yeast extracts" (Sigma), and heated for 10 min at 70°C. After centrifugation at 5 min at 11,200g, 10 µl of supernatant was fractionated by SDS-4-12% NuPAGE, followed by immunoblotting with an appropriate antibody. The antibodies used included anti-ha (Sigma), anti-flag (Stratagene, La Jolla, CA), anti-tubulin (used for loading controls) (Sigma), and anti-^{Nt}Cog1, prepared and purified as described below. Immunoblots were processed using secondary antibodies labeled with different fluorophores. Visualized protein bands were quantified using the Odyssey Imaging System (Li-Cor, Lincoln, NE). The near-infrared fluorescence range and other features of the Odyssey scanner facilitate quantification of immunoblots.

All immunoblotting experiments (Figures 1-5, S3-S5) involved, in addition to explicitly shown data, specific loading controls that utilized immunoblotting with an antibody to tubulin (Hwang et al., 2010b) as shown in Figure 5A, and/or the staining of membranes with Coomassie after protein transfer.

^{35}S-Pulse-Chase Degradation Assays

These experiments were performed essentially as described previously (Hwang et al., 2009; Hwang et al., 2010a; Hwang et al., 2010b). Unless stated otherwise, *S. cerevisiae* strains were grown at 30°C to A_{600} of ~1 in 10 ml of SD medium with components required for auxotrophic growth. Cells were pelleted by centrifugation, gently resuspended, and washed in 0.8 ml of SD medium with required amino acids but without L-Met and L-Cys. Cell pellets were gently resuspended again in 0.4 ml of the same medium and labeled for 5 min at 30°C with 0.16 mCi of ^{35}S-EXPRESS (Perkin-Elmer). Cells were pelleted again and resuspended in 0.3 ml of SD medium containing unlabeled 10 mM L-Met, 5 mM unlabeled L-Cys, and required amino acids. Samples (0.1 ml) were taken at the indicated time points, followed by preparation of extracts by bead beating (FastPrep, 20 seconds at 6.5 M/s, 4 times each), immunoprecipitation with anti-flag magnetic beads (Sigma), SDS-4-12% NuPAGE, electrophoretic transfer of proteins to a PVDF membrane (Invitrogen) and autoradiography. Quantification of ^{35}S-pulse-chases was carried out using Storm PhosphorImager and ImageQuant (GE Healthcare, Pittsburgh, PA).

Antibody Specific for Nt-Acetylated Cog1

Ac-MDEVLPLFRDS, the Nt-acetylated N-terminal peptide of MD-Cog1^{wt}, was used to produce a rabbit antibody, termed anti-Cog1^{AcNt}, that recognized Ac-MDEVLPLFRDS but not its unacetylated counterpart (Figures 1E-H and S4A-C). The Nt-acetylated synthetic peptide AcMDEVLPLFRDSC and its unacetylated counterpart MDEVLPLFRDSC (they bore C-terminal

Cys for crosslinking these peptides to the keyhole limpet hemocyanin carrier protein) were synthesized and purified by Abgent (San Diego, CA). Standard procedures were employed by Abgent to produce rabbit antisera to AcMDEVLPLFRDSC. The resulting antibody (its IgG fraction, produced using immobilized Protein A) was affinity-purified, "positively" at first, against the immobilized AcMDEVLPLFRDSC peptide. The peptide-bound antibody was eluted and thereafter "negatively" purified against the MDEVLPLFRDSC peptide (immobilized using SulfoLink Coupling Resin (Pierce)), with collection, this time, of the unbound antibody fraction. The resulting antibody, termed anti-^{AcNt}Cog1, was highly specific for Nt-acetylated MD-Cog1^{wt} (see Results). Immunoblotting with anti-^{AcNt}Cog1 (1:500 dilution) was carried out for 3 h at room temperature (RT) in 5% skim milk in PBST (PBS containing 0.5% Tween-20). The bound anti-^{AcNt}Cog1 was detected using the Odyssey Imaging System and a goat anti-rabbit antibody (at 1:5,000 dilution) that was conjugated to IRDye-800 (Li-Cor).

Partitioning of Nt-Acetylated and Unacetylated MD-Cog1^{wt} Between Membranes and Cytosol

This assay (Figure S4D-F) used a slight modification of the previously described procedure (Fotso et al., 2005). Wild-type and *naa20Δ* (*nat3Δ*) *S. cerevisiae* expressing MD-Cog1^{wt} (C-terminally tagged with three flag epitopes) were grown at 30°C in 200 ml of SD to A_{600} between 1 and 2. Cells were collected by centrifugation and washed twice with ice-cold distilled water. Cells were disrupted in 1 ml of lysis buffer (1 mM dithiothreitol (DTT), 20 mM HEPES, (pH 7.0), 1 mM PMSF, and protease inhibitor cocktail (Sigma)), using 1 ml of glass beads and vortexing 3 times for 1 min each. The extract was clarified by centrifugation at 3000*g* for 5 min, followed by centrifugation in the TL100 ultracentrifuge (Beckman) at 150,000*g* for 1 h to obtain crude "cytosolic" (supernatant) and "membrane" (pellet) fractions. Membrane fractions were resuspended in 1 ml of Tris-Buffered Saline (TBS). Total clarified extracts and equal total protein amounts of cytosolic and membrane fractions (as determined by the Bradford assay) were fractionated by SDS-4-12% NuPAGE (Invitrogen), followed by immunoblotting with anti-flag antibody. The relative amounts of MD-Cog1^{wt} in cytosolic and membrane fractions were quantified using the Odyssey Imaging System.

Coimmunoprecipitation of Cog1 with Cog3 and Cog4

Wild-type and *naa20Δ* (*nat3Δ*) *S. cerevisiae* expressing specific combinations of either vector alone, MD-Cog1^{wt} (C-terminally tagged with three flag epitopes), Cog3 (C-terminally ha-tagged), or Cog4 (C-terminally ha-tagged) (Figure S4G, H) were grown at 30°C to A_{600} of ~1 in 50 ml of SD containing or lacking appropriate metabolic markers. Cells were collected by centrifugation and resuspended in 0.8 ml of lysis buffer (0.1% NP-40, 10% glycerol, 0.1 M NaCl, 0.5 mM EDTA, 25 mM HEPES, pH 7.5) containing 1X protease inhibitor cocktail and 1 mM PMSF. Cells were disrupted using the FastPrep lysing matrix and bead beating (FastPrep). The extract was clarified by centrifugation at 12,000*g* for 15 min at 4°C. The total protein concentration was measured by the Bradford assay. Equal amounts of total protein were incubated with anti-flag magnetic beads (Sigma) for 2 hrs at 4°C. The beads were washed 3 times with lysis buffer, followed by the elution of beads-bound proteins with 12 µl of 2X NuPAGE LDS sample buffer (containing lithium dodecyl sulfate instead of SDS) with protease inhibitors. Sample were heated at 95°C for 5 min, clarified by centrifugation, and fractionated by SDS-4-12% NuPAGE, followed by immunoblotting with anti-ha antibody and thereafter with anti-flag antibody.

Assays with Protease Inhibitors

MD-Cog1^{wt} C-terminally tagged with three flag epitopes was expressed from the low copy plasmid pRS316Cup1-Cog1-3flag and its P_{CUP1} promoter in *pdr5Δ S. cerevisiae* (the absence of the Pdr5 pump in this mutant allowed for the intracellular retention of MG132, a proteasome inhibitor). Cells were incubated for 1 hr in SD medium containing either 0.5% dimethylsulfoxide (DMSO) (the solvent for a stock solution of MG132), or both 50 μM MG132 and 0.5% DMSO. The incubation was followed by preparation of extracts, SDS-PAGE and immunoblotting with anti-flag antibody. The same procedures were employed using *erg6Δ S. cerevisiae* to examine effects of phenylmethylsulfonyl fluoride (PMSF), an inhibitor of serine proteases, on the degradation of MD-Cog1^{wt}. Cells were incubated either in the presence of 1% isopropanol (the solvent for a stock solution of PMSF), or both 1 mM PMSF and 1% isopropanol, followed by preparation of extracts, SDS-PAGE and immunoblotting with anti-flag antibody (Figure S3D-F).

Table S1: *S. cerevisiae* Strains Used in This Study

Strain	Relevant Genotype	Source
BY4742	*MATα his3-1 leu2-0 lys2-0 ura3-0 can1-100,*	Open Biosystems
BY10976	*ard1Δ::KanMX6 in* BY4742	Open Biosystems
BY15470	*mak3Δ::KanMX6 in* BY4742	Open Biosystems
BY15546	*nat3Δ::KanMX6 in* BY4742	Open Biosystems
BY17299	*doa10Δ:KanMX6 in* BY4742	Open Biosystems
BY4741	*MATa his3-1 leu2-0 met15-0 ura3-0*	Open Biosystems
BY4425	*rad6Δ:: KanMX4* in BY4741	Open Biosystems
BY14589	*cog1Δ::KanMX4* in BY4742	Open Biosystems
ASY101	COG1-3HA::HIS3MX6 in BY4742	This Study
ASY102	COG1-3HA::HIS3MX6 in BY17299	This Study
ASY103	COG1-3HA::HIS3MX6 in BY15546	This Study
ASY105	COG1-13MYC::HIS3MX6 in BY4742	This Study
YW05	*ubc1Δ:: HIS3* JD52	T. Sommers lab collection
BY4454	*mms2Δ::KanMX6* in BY4741	Open Biosystems
BY3994	*ubc5Δ::KanMX6* in BY4741	Open Biosystems
BY3219	*ubc4Δ::KanMX6* in BY4741	Open Biosystems
BBY67.3	*ubc6Δ::HIS3* in JD52	Varshavsky lab collection
BY597	*ubc7Δ::KanMX6* in BY4741	Open Biosystems
BY6577	*ubc8Δ:: KanMX6* in BY4741	Open Biosystems
BY4763	*ubc10Δ:: KanMX6* in BY4741	Open Biosystems
BY1636	*ubc11Δ:: KanMX6* in BY4741	Open Biosystems
BY5214	*ubc12Δ:: KanMX6* in BY4741	Open Biosystems
BY4027	*ubc13Δ:: KanMX6* in BY4741	Open Biosystems
AS104	*ubc6Δ::HIS3, ubc7Δ::KanMX6* in JD52	This Study
BY10568	*erg6Δ::KanMX6* in BY4742	Open Biosystems
RJD3268	*MATa, uba1::KANMX [pRS313 - UBA1-HIS], can1-100, leu2-3, -112, his3-11, -15, trp1-1, ura3-1, ade2-1*	(Ghaboosi and Deshaies, 2007)
RJD3269	*MATa, uba1*Δ::*KanMX* [*pRS313-uba1-204-HIS*], *can1-100, leu2-3, -112, his3-11, -15, trp1-1, ura3-1, ade2-1*	(Ghaboosi and Deshaies, 2007)
JD52	*MATa trp1- 63 ura3-52 his3- 200 leu2-3112. lys2-801*	(Hwang et al., 2010b)
CHY49	*pdr5Δ::KanMX6 in JD52*	(Dohmen et al., 1995)
CHY345	*ubr1Δ::LEU2* in BY4742	This Study
CHY346	*ubr1Δ::LEU2 doa10Δ::KANMX6* in BY4742	This Study
AS106	*not4Δ::HIS3MX6* in BY4742	This Study
AS107	*not4Δ::HIS3MX6 doa10Δ::KANMX6* in BY4742	This Study
AS108	*not4Δ::HIS3MX6 ubr1Δ::LEU2* in BY4742	This Study

Table S2: Plasmids Used in This Study

Plasmid	Description	Source
p316Cup1	pRS316 with P_{CUP1} promoter	This study
p313Cup1	pRS313 with P_{CUP1} promoter	This study
pAS101	Cog1-3flag in p316CUP1	This study
pAS117	MPCog1-3flag in p316Cup1	This study
pAS102	Cog2-3flag in p316CUP1	This study
pAS103	Cog1-3flag in p313CUP1	This study
pAS104	Cog1-3HA in p316CUP1	This study
pAS105	Cog1-HA in p316CUP1	This study
pAS106	Cog3-HA in p316CUP1	This study
pAS107	Cog4-HA in p316CUP1	This study
pAS108	Cog5-HA in p316CUP1	This study
pAS109	Cog6-HA in p316CUP1	This study
pAS110	Cog8-HA in p316CUP1	This study
pAS111	Cog1-3flag in p425GAL1	This study
p413MET25	pRS413 with P_{MET25} promoter	(Mumberg et al., 1994)
pAS112	Hcn1-3flag in p423CUP1	This study
pAS113	Hcn1-3flag in p413MET25	This study
p425Gal1	pRS425 with P_{GAL1} promoter	(Mumberg et al., 1994)
pAS114	Cut9-3flag in p425GAL1	This study
pAS115	Cog2-3flag, Cog3-HA in p423GAL1,10	This study
pAS116	Cog4-HA in p425GAL1,10	This study
pAS118	Cog1-3flag in YEPlac181 with pAdh1	This study
YEPlac181	2μ LEU2 plasmid	Varshavsky lab collection

SUPPLEMENTAL REFERENCES

Arnesen, T., Van Damme, P., Polevoda, B., Helsens, K., Evjenth, R., Colaert, N., Varhaug, J.E., Vandekerckhove, J., Lillehaug, J.R., Sherman, F., *et al.* (2009). Proteomics analyses reveal the evolutionary conservation and divergence of N-terminal acetyltransferases from yeast to humans. Proc Natl Acad Sci USA *106*, 8157-8162.

Ausubel, F.M., Brent, R., Kingston, R.E., Moore, D.D., Smith, J.A., Seidman, J.G., and Struhl, K. (2010). Current Protocols in Molecular Biology. (New York: Wiley-Interscience).

Brower, C.S., and Varshavsky, A. (2009). Ablation of arginylation in the mouse N-end rule pathway: loss of fat, higher metabolic rate, damaged spermatogenesis, and neurological perturbations. PLoS ONE *4*, e7757.

Byrd, C., Turner, G.C., and Varshavsky, A. (1998). The N-end rule pathway controls the import of peptides through degradation of a transcriptional repressor. EMBO J *17*, 269-277.

Choi, W.S., Jeong, B.-C., Joo, Y.J., Lee, M.-R., Kim, J., Eck, M.J., and Song, H.K. (2010).

Structural basis for the recognition of N-end rule substrates by the UBR box of ubiquitin ligases. Nat Struct Mol Biol *17*, 1175-1181.

Dohmen, R.J., Stappen, R., McGrath, J.P., Forrová, H., Goffeau, A., and Varshavsky, A. (1995). An essential yeast gene encoding a homolog of ubiquitin-activating enzyme. J Biol Chem *270*, 18099-18109.

Dougan, D.A., Micevski, D., and Truscott, K.N. (2011). The N-end rule pathway: from recognition by N-recognins to destruction by AAA+ proteases. Biochim Biophys Acta *1823*, 83-91.

Eisele, F., and Wolf, D.H. (2008). Degradation of misfolded proteins in the cytoplasm by the ubiquitin ligase Ubr1. FEBS Lett *582*, 4143-4146.

Fotso, P., Koryakina, Y., Pavliv, O., Tsiomenko, A.B., and Lupashin, V.V. (2005). Cog1p plays a central role in the organization of the yeast conserved oligomeric Golgi complex. J Biol Chem *280*, 27613-27623.

Ghaboosi, N., and Deshaies, R.J. (2007). A conditional yeast E1 mutant blocks the ubiquitin proteasome pathway and reveals a role for ubiquitin conjugates in targeting Rad23 to the proteasome. Mol Biol Cell *18*, 1953-1963.

Gibbs, D.J., Lee, S.C., Isa, N.M., Gramuglia, S., Fukao, T., Bassel, G.W., Correia, C.S., Corbineau, F., Theodoulou, F.L., Bailey-Serres, J., *et al.* (2011). Homeostatic response to hypoxia is regulated by the N-end rule pathway in plants. Nature *479*, 415-418.

Graciet, E., and Wellmer, F. (2010). The plant N-end rule pathway: structure and functions. Trends Plant Sci *15*, 447-453.

Heck, J.W., Cheung, S.K., and Hampton, R.Y. (2010). Cytoplasmic protein quality control degradation mediated by parallel actions of the E3 ubiquitin ligases Ubr1 and San1. Proc Natl Acad Sci USA *107*, 1106-1111.

Helbig, A.O., Gauci, S., Raijmakers, R., van Breukelen, B., Slijper, M., Mohammed, S., and Heck, A.J.R. (2010). Profiling of N-acetylated protein termini provides in-depth insights into the N-terminal nature of the proteome. Mol Cell Proteom *9*, 928-939.

Hu, R.-G., Sheng, J., Xin, Q., Xu, Z., Takahashi, T.T., and Varshavsky, A. (2005). The N-end rule pathway as a nitric oxide sensor controlling the levels of multiple regulators. Nature *437*, 981-986.

Hu, R.-G., Wang, H., Xia, Z., and Varshavsky, A. (2008). The N-end rule pathway is a sensor of heme. Proc Natl Acad Sci USA *105*, 76-81.

Hwang, C.-S., Shemorry, A., and Varshavsky, A. (2009). Two proteolytic pathways regulate DNA repair by co-targeting the Mgt1 alkylguanine transferase. Proc Natl Acad Sci USA *106*, 2142-2147.

Hwang, C.-S., Shemorry, A., and Varshavsky, A. (2010a). The N-end rule pathway is mediated by a complex of the RING-type Ubr1 and HECT-type Ufd4 ubiquitin ligases. Nat Cell Biol *12*, 1177-1185.

Hwang, C.-S., Shemorry, A., and Varshavsky, A. (2010b). N-terminal acetylation of cellular proteins creates specific degradation signals. Science *327*, 973-977.

Hwang, C.-S., Sukalo, M., Batygin, O., Addor, M.C., Brunner, H., Aytes, A.P., Mayerle, J., Song, H.K., Varshavsky, A., and Zenker, M. (2011). Ubiquitin ligases of the N-end rule pathway: assessment of mutations in UBR1 that cause the Johanson-Blizzard syndrome. PLoS One *6*, e24925.

Hwang, C.-S., and Varshavsky, A. (2008). Regulation of peptide import through phosphorylation of Ubr1, the ubiquitin ligase of the N-end rule pathway. Proc Natl Acad Sci USA *105*, 19188-19193.

Kurosaka, S., Leu, N.A., Zhang, F., Bunte, R., Saha, S., Wang, J., Guo, C., He, W., and Kashina, A.

(2010). Arginylation-dependent neural crest cell migration is essential for mouse development. PLoS Genet *6*, e1000878.

Kwon, Y.T., Kashina, A.S., Davydov, I.V., Hu, R.-G., An, J.Y., Seo, J.W., Du, F., and Varshavsky, A. (2002). An essential role of N-terminal arginylation in cardiovascular development. Science *297*, 96-99.

Lee, M.J., Kim, D.E., Zakrzewska, A., Yoo, Y.D., Kim, S.H., Kim, S.T., Seo, J.W., Lee, Y.S., Dorn, G.W., 2nd, Oh, U., *et al.* (2012). Characterization of arginylation branch of the N-end rule pathway in G-protein-mediated proliferation and signaling of cardiomyocytes. J Biol Chem *287*, 24043-24052.

Lee, M.J., Tasaki, T., Moroi, K., An, J.Y., Kimura, S., Davydov, I.V., and Kwon, Y.T. (2005). RGS4 and RGS5 are in vivo substrates of the N-end rule pathway. Proc Natl Acad Sci USA *102*, 15030-15035.

Lees, J.A., Yip, C.K., Walz, T., and Houghton, F.M. (2010). Molecular organization of the COG vesicle tethering complex. Nat Struct Mol Biol *11*, 1292-1298.

Licausi, F., Kosmacz, M., Weits, D.A., Giuntoli, B., Giorgi, F.M., Voesenek, L.A.C.J., Perata, P., and van Dongen, J.T. (2011). Oxygen sensing in plants is mediated by an N-end rule pathway for protein destabilization. Nature *479*, 419-422.

Longtine, M.S., McKenzie, A., 3rd., Demarini, D.J., Shah, N.G., Wach, A., Brachat, A., Philippsen, P., and Pringle, J.R. (1998). Additional modules for versatile and economical PCR-based gene deletion and modification in Saccharomyces cerevisiae. Yeast *14*, 953-961.

Matta-Camacho, E., Kozlov, G., Li, F.F., and Gehring, K. (2010). Structural basis of substrate recognition and specificity in the N-end rule pathway. Nat Struct Mol Biol *17*, 1182-1188.

Miller, V.J., and Ungar, D. (2012). Re'COG'nition at the Golgi. Traffic *13*, 891-897.

Mogk, A., Schmidt, R., and Bukau, B. (2007). The N-end rule pathway of regulated proteolysis: prokaryotic and eukaryotic strategies. Trends Cell Biol *17*, 165-172.

Mumberg, D., Muller, R., and Funk, M. (1994). Regulatable promoters of Saccharomyces cerevisiae - comparison of transcriptional activity and their use for heterologous expression. Nucleic Acids Res *22*, 5767-5768.

Piatkov, K.I., Brower, C.S., and Varshavsky, A. (2012a). The N-end rule pathway counteracts cell death by destroying proapoptotic protein fragments. Proc Natl Acad Sci USA *109*, E1839-E1847.

Piatkov, K.I., Colnaghi, L., Bekes, M., Varshavsky, A., and Huang, T.T. (2012b). The auto-generated fragment of the Usp1 deubiquitylase is a physiological substrate of the N-end rule pathway. Mol Cell *48*, 926-933.

Polevoda, B., Arnesen, T., and Sherman, F. (2009). A synopsis of eukaryotic N-terminal acetyltransferases: nomenclature, subunits and substrates. BMC Proceedings *3*, S2.

Polevoda, B., and Sherman, F. (2003). N-terminal acetyltransferases and sequence requirements for N-terminal acetylation of eukaryotic proteins. J Mol Biol *325*, 595-622.

Prasad, R., Kawaguchi, S., and Ng, D.T.W. (2010). A nucleus-based quality control mechanism for cytosolic proteins. Mol Biol Cell *21*, 2117-2127.

Rao, H., Uhlmann, F., Nasmyth, K., and Varshavsky, A. (2001). Degradation of a cohesin subunit by the N-end rule pathway is essential for chromosome stability. Nature *410*, 955-960.

Sasidharan, R., and Mustroph, A. (2011). Plant oxygen sensing is mediated by the N-end rule pathway: a milestone in plant anaerobiosis. Plant Cell *23*, 4173-4183.

Sherman, F. (1991). Getting started with yeast. Meth Enzymol *194*, 3-21.

Starheim, K.K., Gevaert, K., and Arnesen, T. (2012). Protein N-terminal acettyltransferases: when the start matters. Trends Biochem Sci *37*, 152-161.

Sztul, E., and Lupashin, V. (2009). Role of vesicle tethering factors in the ER-Golgi membrane

traffic. FEBS Lett *583*, 3770-3783.

Tasaki, T.S., Sriram, S.M., Park, K.S., and Kwon, Y.T. (2012). The N-end rule pathway. Annu Rev Biochem *81*, 261-289.

Turner, G.C., Du, F., and Varshavsky, A. (2000). Peptides accelerate their uptake by activating a ubiquitin-dependent proteolytic pathway. Nature *405*, 579-583.

Van Damme, P., Lasac, M., Polevoda, B., Gazquezc, C., Elosegui-Artolae, A., Kim, D.S., De Juan Pardoe, E., Demeyera, K., Holef, K., Larreac, E., *et al.* (2012). N-terminal acetylome analyses and functional insights of the N-terminal acetyltransferase NatB. Proc Natl Acad Sci USA *109*, 12449-12454.

Varshavsky, A. (1996). The N-end rule: functions, mysteries, uses. Proc Natl Acad Sci USA *93*, 12142-12149.

Varshavsky, A. (2011). The N-end rule pathway and regulation by proteolysis. Prot Sci *20*, 1298-1345.

Wang, H., Piatkov, K.I., Brower, C.S., and Varshavsky, A. (2009). Glutamine-specific N-terminal amidase, a component of the N-end rule pathway. Mol Cell *34*, 686-695.

Xia, Z., Turner, G.C., Hwang, C.-S., Byrd, C., and Varshavsky, A. (2008a). Amino acids induce peptide uptake via accelerated degradation of CUP9, the transcriptional repressor of the PTR2 peptide transporter. J Biol Chem *283*, 28958-28968.

Xia, Z., Webster, A., Du, F., Piatkov, K., Ghislain, M., and Varshavsky, A. (2008b). Substrate-binding sites of UBR1, the ubiquitin ligase of the N-end rule pathway. J Biol Chem *283*, 24011-24028.

Zenker, M., Mayerle, J., Lerch, M.M., Tagariello, A., Zerres, K., Durie, P.R., Beier, M., Hülskamp, G., Guzman, C., Rehder, H., *et al.* (2005). Deficiency of UBR1, a ubiquitin ligase of the N-end rule pathway, causes pancreatic dysfunction, malformations and mental retardation (Johanson-Blizzard syndrome). Nat Genet *37*, 1345-1350.

Zhang, F., Saha, S., Shabalina, S.A., and Kashina, A. (2010a). Differential arginylation of actin isoforms is regulated by coding sequence-dependent degradation. Science *329*, 1534-1537.

Zhang, Z., Kulkarni, K., Hanrahan, S.J., Thompson, A.J., and Barford, D. (2010b). The APC/C subunit Cdc16/Cut9 is a contiguous tetratricopeptide repeat superhelix with a homodimer interface. EMBO J *29*, 3733-3744.